J. Water Environ. Nanotechnol., 8(2): 151-163 Spring 2023

ORIGINAL RESEARCH PAPER

An Examination of the Application of Polyurethane-Based Hydrophobic Nanocoatings Inspired by Natural Structures in Extracting Water from Air Humidity

Ashkan Zolriasatein*[*1], Sepideh Abdollahzadeh[2], Negar Motakef Kazemi[2]

[1]Non-metallic Materials Research Department, Niroo Research Institute, Tehran, Iran
[2]Islamic Azad University of Tehran, Tehran, Iran

Received: 2022-11-14 Accepted: 2023-01-14 Published: 2023-05-20

ABSTRACT
Nowadays, water shortage has become a severe issue all over the world, especially in some arid and undeveloped areas. Water is a renewable natural resource that can produce freshwater globally. Interestingly, some animals in nature can collect water from fog, which can be the inspiration to develop novel and functional water-collecting materials. A superhydrophobic surface that utilizes no energy has been synthesized from a water-collecting mechanism of the Stenocara beetles back structures. Firstly, this paper reviews the preparation methods of superhydrophobic surface coatings and later examines patterns inspired by nature. In this paper, hydrophobic nanocoating was manufactured based on polyurethane (PUR) modified by nano-silica. Silica nanoparticles were synthesized via the sol-gel method. Then, silica nanoparticles were dispersed in polyurethane (PU) coatings. In this article, many factors of collecting moisture are evaluated, for example, temperature, pattern placement angle, pattern shape, types of surface patterns, and ambient humidity. Finally, are introduced the optimum situation for absorbing water from the fog.

Keywords: hydrophobic, nanocoating, polyurethane, sol-gel, Stenocara beetles

How to cite this article
Zolriasatein A., Abdollahzadeh S., Motakef Kazemi N., An Examination of the Application of Polyurethane-Based Hydrophobic Nanocoatings Inspired by Natural Structures in Extracting Water from Air Humidity. J. Water Environ. Nanotechnol., 2023; 8(2): 151-163 DOI: 10.22090/jwent.2023.02.005

INTRODUCTION

Freshwater scarcity is increasingly perceived as a global systemic risk. Two-thirds of the world's lands are experiencing water scarcity, especially in semi-arid and desert regions. Atmospheric water and fog constitute approximately 10% of all fresh water on Earth [1]. Wastewater reuse can therefore be a valuable option for water supply in areas where water is limited. Air humidity could be a potential renewable source. The classic wastewater treatment system includes conventional physical, chemical, and biological methods; but each of these approaches has some limitations. 2-Nitrophenol (2NP) is a poisonous and bio refractory contaminant in petrochemical wastewater which can cause significant injury to the environment and human health based on its high solubility and stability in water [2]. The existence of the nitro group on phenolic rings makes it more resistant to chemical and biological treatment methods [3]. The remediation of wastewater polluted with nitrophenols by traditional methods is difficult. 2-Nitrophenol is considered to be a hazardous waste and toxic contaminant by U.S. Environmental Protection Agency (EPA) [4]. Abstract—Removal of 2-nitrophenol (2NP) from an aqueous solution was performed using the Sono-Fenton process. The Box–Behnken design (BBD) of experiments was used to investigate the influence of operational factors such as pH, initial concentration of hydrogen peroxide, and ferrous ions on the removal of 2NP [5].

* Corresponding Authors Email: *azolriasatein@nri.ac.ir*

Thus, collecting tiny water droplets or fog could help overcome global water shortages [6]. In recent years, controlling dropwise condensation for water collection found extensive application prospects in various industries, including water treatment or recovery in power stations [7], seawater desalination [8], heat transfer [9], microfluidic devices [10] and others. In nature, the Darkling beetle (Stenocara gracilipes of Tenebrionidae family), also known as fog stand beetle, is a species of beetle that is native to the Namib Desert of southern Africa, which absorbs water in the atmosphere through the hydrophilic protrusions of its shell surfaces and then transports it to the mouth through the hydrophobic groove to supply water resources. Inspired by the shell structure of this desert beetle species, a large number of scholars have prepared various biomimetic structure surfaces that combined super hydrophilic/hydrophilic and superhydrophobic/hydrophobic regions. These so-called hybrids super wettable (HSW) surfaces have broad application prospects in water/fog harvesting [11-14].

At present, there are numerous methods of HSW surface preparation, such as reactive ion etching [15-16], laser processing [17], photocatalysis [18], and others. Hou et al. fabricated superhydrophobic surfaces with an array of superhydrophobic patterns using lithography and deep reactive ion etching technology. These surfaces were found to enhance the dropwise condensation effect and to have an excellent droplet-stripping effect and heat exchange performance. Mahapatra et al. [19] used carbon dioxide laser-processing techniques to create patterns on superhydrophobic aluminum surfaces, which promoted the condensation of droplets on these surfaces. Bai et al. [20] designed super hydrophilic star-shaped patterns using the mask photocatalysis technology for the titanium dioxide (TiO_2) superhydrophobic surface, which patterns enhanced the water collection effect of the surface. Zhu and Guo [21] fabricated a titanium dioxide-copper (TiO_2-Cu) composite surface modified with thiol and produced an HSW surface with excellent water collection efficiency and outstanding abrasion resistance. According to recent studies, hybrid HSW surfaces with super hydrophilic and superhydrophobic parts have considerable advantages regarding condensation, water harvesting, and heat exchange over more conventional surface structures. Therefore, it is also a vital issue in the field of bionic materials to develop a low-cost, readily prepared HSW surface. The surface of TiO_2 modified by a low-surface-energy substance such as fluoro-alkyl silanes (FAS) can become superhydrophobic [22]. Due to the excellent photocatalytic properties of TiO_2, the FAS monolayer deposited on the surface of TiO_2 can be catalytically decomposed by UV irradiation [23]. This leads to a wetting transformation of the TiO_2 surface. On the contrary, the decomposition of FAS monolayer modified on the surface of silicon dioxide (SiO_2) nanoparticles is hard to achieve by UV irradiation. Given this, an HSW surface with mixed super hydrophilic TiO_2 and superhydrophobic SiO_2 nanoparticles can be produced by maskless UV irradiation. To the best of the authors' knowledge, this is the first attempt to apply maskless photocatalysis to the fabrication of HSW surfaces for water harvesting.

Today, the only industrial-scale device for fog harvesting is the polymer mesh installation, which is now available in many dry areas of the world [24]. One of the most important parameters in fog harvesting techniques is the hydrophobicity of the collector. Polypropylene, polyethylene, nylon, and stainless steels with different hydrophobicity grades are examples of the materials used for this purpose. Superhydrophobic materials, which have attracted attention in recent years, have the properties such as self-cleaning, stain retention, and antifouling [25].

To produce such superhydrophobic surfaces; the sol-gel process, chemical vapor deposition, lithography, chemical etching, and electrospinning methods were used [26-27]. Electrospinning is a simple method that can be used to obtain the necessary structure. The porous film using hydrophilic polymer or containing hygroscopic nanoparticles can capture water droplets from the moist air due to their high specific surface area. Production involves the random delivery of a hydrophilic material onto a hydrophobic surface. However, this method is not suitable for repeated production [28-29]. Although the lithography method can accurately produce pre-designed patterns, it is not preferred due to its disadvantages such as the difficulty in controlling the process and the use of hazardous chemicals [30-31]. Ink-jet printing is a one-step procedure, but expensive. For all these reasons, low-cost methods are required for practical applications along with high fog harvesting efficiency.

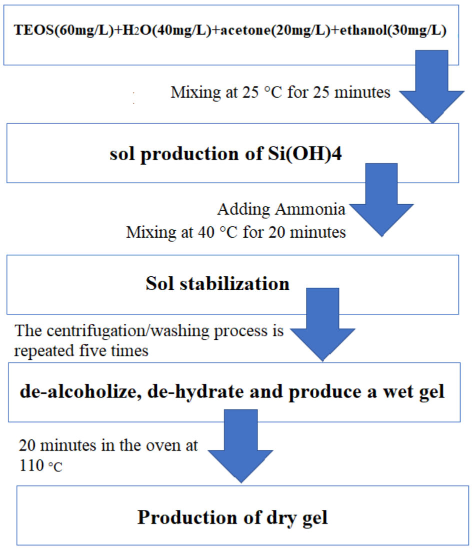

Fig. 1: Synthesis of silica nanoparticles by modified sol-gel process

It has been reported that the fog-harvesting ability of polyethylene terephthalate fibers is affected by the cross-section and surface structure [32]. Also, silicone elastomers and fluoropolymers are widely used in the preparation of superhydrophobic surfaces [33-34]. Polyacrylonitrile is a stable polymer that is widely used as a raw material in the process of functionalization with its good mechanical and chemical properties [35]. Recently, various microfabrication and chemical treatment strategies have been developed to produce polydopamine-coated bumps, titanium dioxide nanoparticles, and Trigonella foenum graecum on a hydrophobic surface [36-37]. In addition, it was found that almost all of the rough areas on the surface of various insect species were covered with a wax layer and this increased the efficiency of fog harvesting [38]. This result brought a new perspective to fog harvesting efforts. It was found that knop-like tissues with convex surfaces maximize the fog condensation rate [39]. The type and the content of nano-silica play significant roles in water uptake. Moreover, the results obtained from the gravimetric method showed that the coatings tend to absorb water rapidly in the initial days. After such periods a further slow increase in water uptake is initiated for hydrophilic-silica-filled coatings [40].

Polyurethane contains block copolymers of a urethane group (—NHCOO—) and a ureido group (—NHCONH—) [41]. This material has the advantages of high strength, wear resistance, and tear resistance. As an adhesive, polyurethane has been widely used in the preparation of superhydrophobic surfaces [42-45]. To create a polyurethane that has a lower surface energy, silicone or organic fluorine is usually used as a modifier. Organic fluorine-modified polyurethane has poor low-temperature resistance and toxicity [46-47], which has great limitations on the promotion and application of fluorine-containing materials. Therefore, silicone has been modified in the present experiment.

In the current study, to achieve a coating with good performance, especially in hydrophobicity, nano SiO_2, fluorine components, and polyacrylate-polyurethane are combined via a copolymerization process followed by cross-linking. A set of techniques including Fourier transform infrared (FTIR) spectroscopy and scanning electron microscopy (SEM). Then, surface hydrophobicity, chemical resistance, and mechanical properties have also been studied. Additionally, amounts of collecting water by nanocoating surfaces based on varieties of natural patterns were checked [48].

MATERIALS AND METHODS

Materials

Silica particle, alcohol, acetone, tetraethyl orthosilicate (TEOS), ammonia solution, methyltriethoxysilane (MTES), octyltriethoxysilane (OTES), vinyltriethoxysilane (VTES), methoxy peroxy silane, butyl acrylate (BA), methyl methacrylate (MMA), 2-hydroxyethyl methacrylate

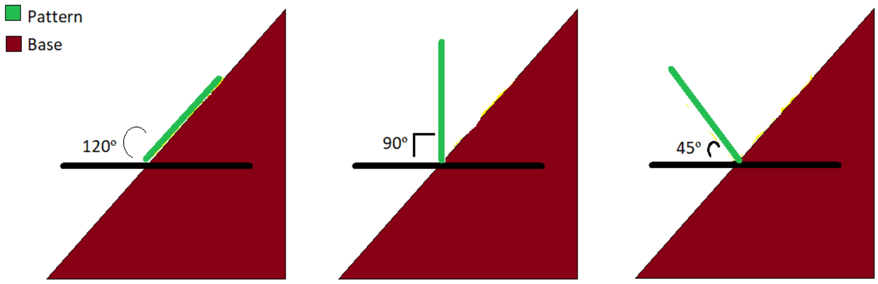

Fig. 2: The design of how samples are placed on angles at 45°, 90° and 120°

(HEMA), 1,6-hexamethylene diisocyanate trimer butyl acetate, t-butyl hydroperoxide (TBHP), dibutyltin dilaurate, styrene (St).

Preparation of polyurethane/silica nano-coating

Silica nanoparticles were synthesized by chemical method from tetraethyl orthosilicate (TEOS) and ethanol (C2H5OH) (Fig. 1).

The ammonia molar ratio is 1:4:8:0.2. The original silica sol obtained is colloidal silica in ethanol, which was exposed respectively to MTES, OTES, VTES, and MATMS at 35°C for 8 hours.

Silane coupling agents with 0.25 mol per 100 parts by weight of silica sol were added to the reaction system.

First, TEOS: 60 mg/L, H2O: 20 mg/L of, acetone: 20 mg/L, and ethanol: 30 mg/L are mixed for 20 minutes with ultrasound at a temperature of 25 °C to create a sol of silica, to produce silica nanoparticles [49].

Ammonia:10 mg/L was added and mixed at 40 °C for 20 min. The concentration of ammonia is the more significant factor in dictating the size of the SiO2 nanoparticles. With the increasing volume of ammonia solution, an increase in the size of silica nanoparticles was observed. [50].

Typically, polymer hydrogels were isolated in manufacturing as wet gels that contain manufacturing impurities such as monomers, initiator residues, salts, solvents, and soluble oligomers. Depending on their intended application, the polymers are purified and dried to the required extent. Drying usually is necessary for the centrifugation/washing process and is repeated five times. The obtained gel is finally oven-dried for 20 minutes at 110 °C.

Next, silica polyurethane nanocoating, polyester-grade polyurethane (pu140A80): 15 gr with silica nanoparticles:15 gr was mixed and obtained by the sol-gel method at room temperature. There were two reasons for choosing the amounts of polyurethane added to silica nanoparticles. First, the obtained nanocoating is transparent and without turbidity. Secondly, it has the property of sticking to surfaces.

Experimental Tests

This nanocoating was examined on the glass and aluminum surfaces. First, to remove dust and oil can be used alcohol and acetone. Then, the nanocoating is applied to surfaces on various patterns with different designs (Fig. 3). The nanocoating is covered where on the middle and edge of the slides. The glass and aluminum slides without nanocoating were chosen for checking tests. Increasing surface roughness is beneficial for improving the hydrophobicity of the coating. So, a glass slide was roughed and then coated by nanocoating.

Another was aluminum surfaces, which were cut to the size of a glass slide (7.5X2.5 cm). All glass slide patterns were repeated on aluminum surfaces. Just in case, soft sandpaper was used for making rough surfaces. In addition to the elementary designs, sheets of aluminum were cut to the size of glass slides and then crumpled and flattened for the aluminum coating coverage.

Relative humidity is a measure of the percentage saturation of the air. Therefore, to prepare the placement of tests was chosen place, at 57% relative humidity in a cold (18±2 °C) and hot (35±2 °C) temperature. In another test, to investigate the effect hydrophobic of nanocoating, the whole surfaces were studied at angles of 45°, 90° and 120° degrees (Fig. 2). Several times, this test was evaluated, immediately after stopping the humidifier, one, two and three hours after that. To ensure nanocoating and the process of tests was performed five times.

Finally, glass and aluminum slides are coated with nano coating in various designs and evaluated in ideal situations. (Fig. 4).

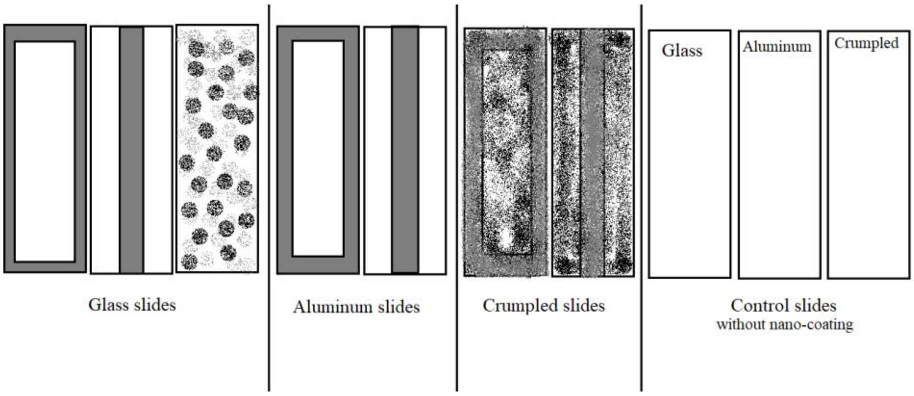

Fig. 3: Primary surface patterns of nanocoating polyurethane/silica

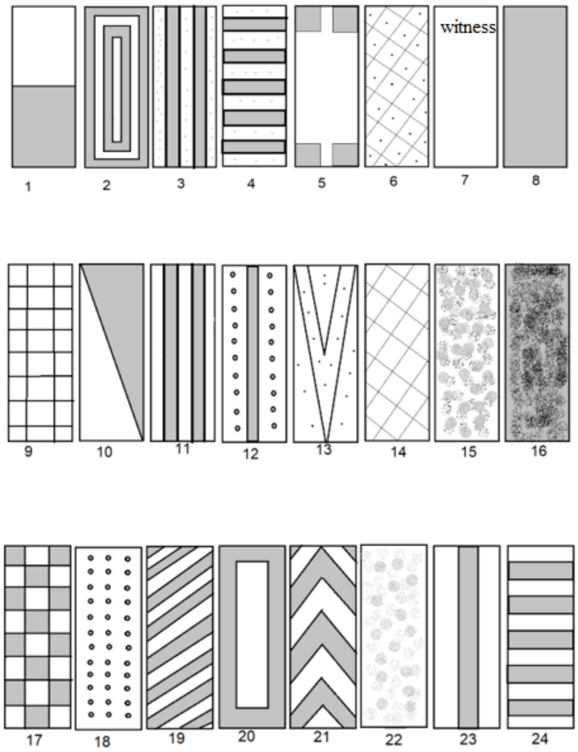

Fig. 4: Nature-inspired patterns to measure the amount of water with the nanocoating polyurethane/silica

Pattern.3 is similar to the elytra of the Namib beetle S.Gracilipes longitudinally. Pattern.4 is identical to pattern.3, with the only difference being in lines that are in cross-sections. Pattern.6 is the same as the elytra of the O.Unguicularis beetle. Pattern.7 surface without nanocoating was used as a control for comparison. Pattern. 8 is another control of the test, which has the nanocoating. Pattern.13 is similar to the surface pattern of the P.Cribripes beetles. Pattern.15 includes a surface that was first sanded in preparation for the placement of the nanocoating. Pattern.16 was covered by the nanocoating and then sanded down (sanding on aluminum, do not possible to apply rough sandpaper on the surface. Soft sandpaper has been used). Pattern.17 was designed checkered. Pattern.18 is similar to a spider's web and was designed with rough puffs. Pattern.22 is without coated and has only been sanded.

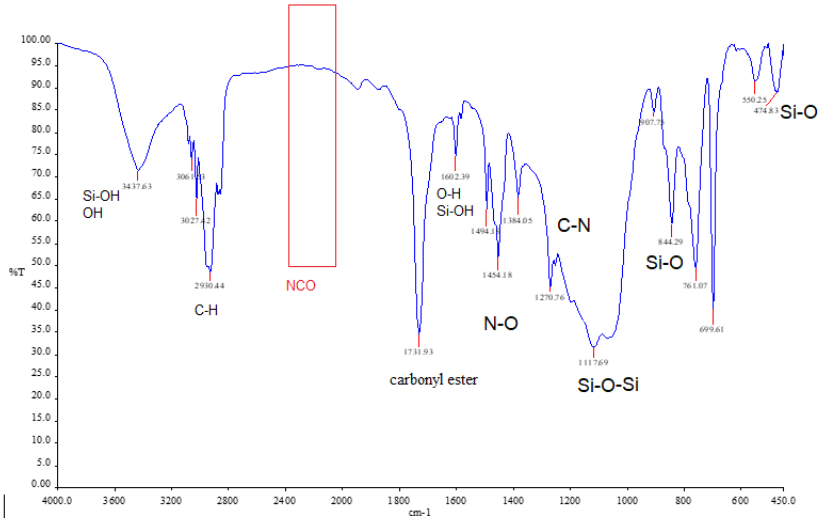

Fig. 5: FT-IR analysis of nanocoating polyurethane/silica

Examining the degradability and stability of the nanocoating

Glass and aluminum slides are covered to check the stability of hydrophobic the nanocoating in different circumstances.

RESULTS AND DISCUSSION

Contact angle results:

To check the contact angle of the nanocoating, glass, and aluminum slides are about 7.5X2.5 cm coated by the nanocoating, and surfaces without nanocoating were controlled again.

The findings of the tests conducted are according to Table 1 performed that the contact angle of the glass surface without nanocoating is equal to 48.2. However, the contact angle of the aluminum surface without nanocoating is 71.3 º, which is more hydrophobic than the glass surface. After covering the nanocoating, the contact angle of glass in a static state is 99.3 º, and in aluminum is 147.6 º. The aluminum surface is a more hydrophobic character. Generally, a superhydrophobic surface was defined as a surface with a high-water contact angle (WCA) greater than 150°.

Experimental dynamic contact angle results of Table 2 showed that glass and aluminum surfaces covered with the nanocoating were 103° and 160°, respectively. Other studies showed that the PEA coating film is somewhat hydrophilic due to the presence of 2-hydroxyethyl acrylate parts in water. Interestingly, the WCA increased from 97.5° for FPEA to 108.0° for SiO_2-FPEA with SiO_2 nanoparticles incorporation [51].

In this examine was observed that the PU/SiO2 nanocoating is super hydrophobic. PU/SiO2 nanocoating is a suitable coating for having adhesion force and structural stability. This produced coating is also resistant to wear. Therefore, both materials have the properties of PU/SiO2 composite super-hydrophobic coating [52]. Surface modification is a suitable method for improving the dispersion of SiO2 nanoparticles.

FT-IR analysis

Fig. 5 shows the FT-IR spectrum of SiO_2 nanoparticles and polyurethane polymer. The peaks are visible clearly. Stretching vibrations Si-O asymmetric is the strong peak at 1117 cm^{-1}. The peak at 844 cm^{-1} and 474 cm^{-1} are attributed to Si-O-Si symmetric stretching vibration absorption and Si-Si-O bending vibration. The characteristics of the absorption peaks of Si and O-H appear respectively at 1602 cm^{-1} and 3437 cm^{-1}. In the absence of peaks at 2800-3000 cm -1 in nano SiO_2, peaks at 2930 and 2965 cm^{-1} appear, which is attributed to C=H, -CH2- stretching vibration. The new peaks observed at 1731 and 1635 cm^{-1} for C=O and C=C are shown. Bending vibration (2200-2400 cm^{-1}) for the Carbonyl ester group appeared characteristic of C-O-C near 1270 and 1150 cm^{-1}. The absence of characteristic absorption of C=C at 1637 cm^{-1} indicates the complete reaction of all monomers in the copolymerization process. The incorporation of silica nanoparticles synthesized is confirmed successfully in the coatings. Comparing the findings with previous articles shows that

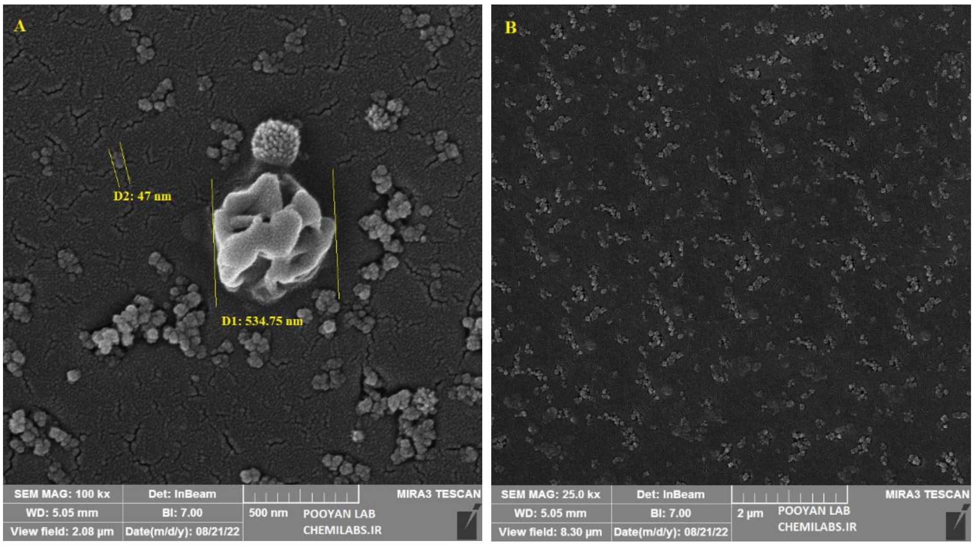

Fig. 6: SEM microscope photo of the produced nano-coating. A) The dispersion of nanocoating is seen clearly. B) Surface image of the nanocoated substrate

Table 1: Static contact angle measurements

Sample	Average CA (Degrees)
Glass slide	48.2 º
Aluminum slide	71.3 º
Nanocoated Glass Slide	99.3 º
Nanocoated Aluminum	147.6 º

Table 2: Measurement of dynamic contact angles

Sample	Average CA (Degrees)
Nanocoated Slide	Avg Adv = 103.0 º Avg Rec = 75.5 HCA=27.5
Nanocoated aluminum	Avg Adv = 160.0 º Avg Rec = 95.5 HCA=27.5

the results obtained from FT-IR are close to the previous results and are confirmed based on the tables related to the spectroscopy of all structure factors in nanocoating [53].

SEM Results

Fig. 6 shows the surface morphology of the nanocoating polyurethane/silica. The surface is smooth, uniform, and without defects (Fig 6-B) and was used as a suitable coating. In the magnified image (Fig 6-A), nanoparticles of SiO_2 with an average size of about 47 nm and a good dispersion index (PDI) of ~0.197 are scattered on the surface of the template and do not cause aggregation. The closely packed SiO_2 nanoparticles formed a dense surface structure with a uniform roughness, probably between 40 and 55 nm, which could act as a protective layer and UV-resistant coating.

Table 3: Water collecting was evaluated based on the placement angle, kinds of designs, and temperatures immediately after stopping the humidifier.

Various Types of Patterns / Types of environments	Cold humidity with a placement angle of 120°	Hot humidity with a placement angle of 120°	Cold humidity with a placement angle of 90°	Hot humidity with a placement angle of 90°	Cold humidity with a placement angle of 45°	Hot humidity with a placement angle of 45°
Glass slide with coating on the edges	65 cc	40 cc	50 cc	30 cc	40 cc	10 cc
Glass slide with coating in the middle part	60 cc	35 cc	45 cc	25 cc	35 cc	5 cc
Sanded glass slide	65 cc	40 cc	45 cc	30 cc	35 cc	10 cc
Aluminum plate with coating on the edges	110 cc	75 cc	90 cc	55 cc	80 cc	35 cc
Aluminum plate with coating in the middle part	95 cc	70 cc	75 cc	50 cc	65 cc	30 cc
Crumpled and smoothed aluminum with coating on the edges	115 cc	100 cc	95 cc	80 cc	85 cc	60 cc
Crumpled and smoothed aluminum with coating in the middle part	90 cc	85 cc	75 cc	65 cc	65 cc	45 cc
Glass without nanocoating	30 cc	25 cc	20 cc	15 cc	10 cc	could not be measured
Aluminum without nanocoating	50 cc	45 cc	35 cc	30 cc	25 cc	10 cc
Crumpled aluminum without nanocoating	55 cc	50 cc	40 cc	35 cc	30 cc	15 cc

Compared to other articles, the nanoparticle of silica is 35 nm. In this Article, due to the production of silica nanoparticles by the sol-gel method and the use of ammonia, the size of nanoparticles is 47 nm has arrived [54].

In other investigations, it was observed that the higher the amount of ammonia in the sol-gel method for stability, the larger the size of the nanoparticles and the higher the porosity in the gel [55].

Experimental tests

The results are shown in Table 3 that the most effect on obtained water including moisture in cold temperatures and patterns placements angle of 120° with designed nanocoating on the edge of the surfaces. The inappropriate situation for collecting the water of fog is that placements f the surface of 45° and warm environments by covered with nano coating in the middle part of surfaces.

Table 3 shows that the volume of water obtained in aluminum without nanocoating is much more than in glass slide in the same qualification.

The results in the Table 4 are similar to those in Table 3. Important parameters for collecting water consist of the placement angle, temperature, and designs of the pattern.

Namib beetle can collect water behind its wings or elytra in the morning fog at 18-20 °C. On the other hand, the Namib beetle has acted similarly to an aluminum plate due to having hydrophilic and hydrophobic ridges and peaks [56].

Some structures made to collect water from air humidity are placed at a zero-degree angle. The remaining consists of plastic patterns for water consumption in agriculture or the Hulk net pattern placement at a 90° angle. This article examines collecting water without energy consumption. So, there are no comparison models with the mentioned.

All surfaces without nanocoating and the nanocoated patterns increased significantly, At the placement angle of 120°. The results observed that the quantity of water obtained in cold temperatures is more than in hot environments. According to data acquired from the Namib beetles, when the

Table 4: Three hours after stopping the humidifier, water collecting was evaluated based on the placement angle, kinds of designs, and temperatures.

Various Types of Patterns / Type of environments	Cold humidity with a placement angle of 120°	Hot humidity with a placement angle of 120°	Cold humidity with a placement angle of 90°	Hot humidity with a placement angle of 90°	Cold humidity with a placement angle of 45°	Hot humidity with a placement angle of 45°
Glass slide with coating on the edges	50 cc	10 cc	35 cc	<5 cc	25 cc	could not be measured
Glass slide with coating in the middle part	40 cc	5 cc	25 cc	could not be measured	15 cc	could not be measured
Sanded glass slide	45 cc	10 cc	30 cc	<5 cc	20 cc	could not be measured
Aluminum plate with coating on the edges	95 cc	45 cc	75 cc	35 cc	65 cc	15 cc
Aluminum plate with coating in the middle part	80 cc	40 cc	60 cc	30 cc	50 cc	10 cc
Crumpled and smoothed aluminum with coating on the edges	100 cc	70 cc	80 cc	60 cc	70 cc	40 cc
Crumpled and smoothed aluminum with coating in the middle part	75 cc	55 cc	55 cc	45 cc	45 cc	25 cc
Glass without nanocoating	20 cc	5 cc	<5 cc	<5 cc	could not be measured	could not be measured
Aluminum without nanocoating	40 cc	20 cc	20 cc	10 cc	10 cc	could not be measured
Crumpled aluminum without nanocoating	45 cc	25 cc	25 cc	15 cc	15 cc	could not be measured

elytra placement angle is at 45° they have moved water, and the speed and movement of the droplet are increased at higher angular [57].

In all tests, the amount of water in the wrinkled aluminum patterns for creating macroscopic topography is more. According to the schematic shape of the wing of the Namib beetles, surface topographies can be produced in nano dimensions using H or fs lasers like the surface pattern of the beetle's wing. For further investigation, variant patterns are designed on glass and aluminum, using schematic shapes in spider webs and points like the Namib beetle wings in surface patterns. Several surface patterns close to nature patterns were prepared and described in Fig. 4. All surfaces have been placement an angle of 120°.

This test was for checking the best-designed pattern. Fig. 7 shows that in the pattern.1, the volume of water obtained is different depending on the kind of placement. The highest and lowest water collected in the glass design is in pattern.2 and 8. Pattern.3 and 4, which are longitudinal and transverse and similar to the wing shape of the S. gracilipes beetle, both obtained water in the same way and there was no difference between transverse and longitudinal shapes.

According to the results of Fig. 8, the lowest water collected is in pattern.13. Pattern.15 and 16 both obtained the same amount of water.

Fig. 9 shows that collecting water in pattern.1 in both ways of placing has been collected water. Patterns.3 and 4 show that the transverse lines collect more water than the longitudinal lines due to the increased sequence between the hydrophobic and hydrophilic surfaces. Pattern.6 is similar to O.unguicularis and obtained more water volume than other designs.

Patterns.15 and 16, the coated nano-coating was removed from the aluminum and obtained less water (Fig. 10).

In this review, compared to other articles, O.unguicularis is only one of the four beetles that consider the standing head fogging mode in a low-temperature environment with artificial fog. The

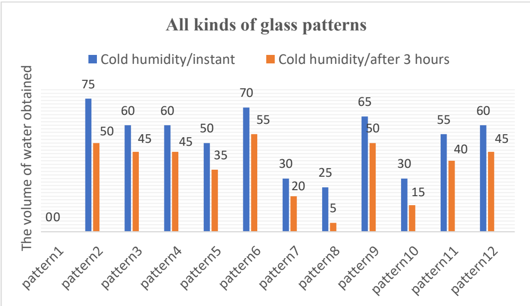

Fig. 7: Examination of different designs on glass at an angle of 120º

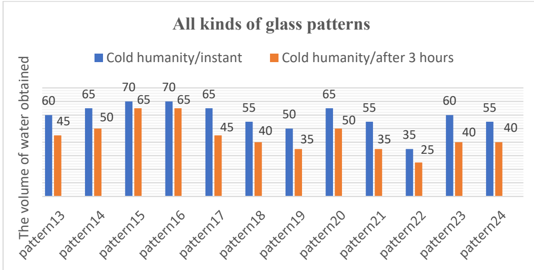

Fig. 8: Examination of different designs on glass at an angle of 120º

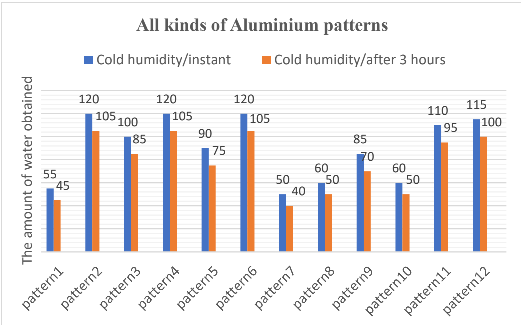

Fig. 9: Examination of different designs on aluminum at an angle of 120º

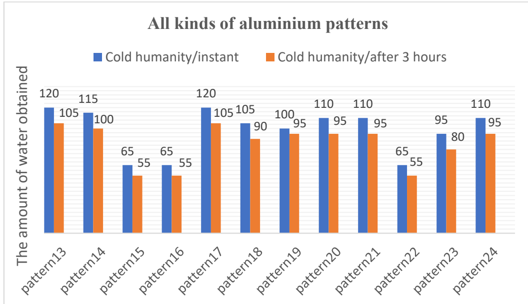

Fig. 10: Examination of different designs on aluminum at an angle of 120º

efficiency of fog removal from the elytra water of fogging and non-fogging beetles shows that S.Gracilipes is small and O.Unguicularis foggers are the better harvesters of fog water. P.cribripes is the largest and worst species of collecting moisture from the air [58].

Based on previous investigations, a super hydrophilic-superhydrophobic pattern inspired by the desert beetle for efficient fog harvesting using a simple spray method and selective modification consisting of a hierarchical hydrophobic microparticle/hydrophilic nanoparticle structure fabricated. As for the Mercaptan, When the mass ratio of Cu_2O microparticles to ZrO_2 nanoparticles in the spray suspension stood at 8:1, the prepared super hydrophilic-superhydrophobic hybrid sample had the highest fog collection efficiency of approximately 1707.25 mg/cm^{-2}/h^{-1}. In other words, at a typical mist velocity of 50 cm/s, the super hydrophilic-superhydrophobic hybrid sample constructed with an area of 1 square meter can collect approximately 17 L of fresh water, which can fully meet the water consumption [59]. The ratio of the surface's size in this research is 7%.

Examining the degradability and stability of the nanocoating

First, all patterns remained in a jar with 70% alcohol. It observed that a stability period was six days. Second, the consistency was three hours when samples were placed in a 3% HCL solution. Patterns were put in an oven at 120 °C. The samples were healthy at 105 °C, and after that, they started to destroy. The main point is that the aluminum surface covered by nanocoating was unstable by scratching.

CONCLUSION

Experimental results showed that the polyurethane/SiO_2 nanocoating, with its high hydrophobic properties, can be collected air humidity without using energy on surfaces.

This study showed that the glass surface has a contact angle of 48.2° and the aluminum surface has a contact angle of 71.3°. The static contact angle of the covered glass is 99.3°, and the dynamic contact angle is 103.0°. In this test for coated aluminum, the static contact angle is 147.6°, and the dynamic contact angle is 160.0°.

Therefore, covered aluminum is a superhydrophobic surface.

SEM analysis, nanocoating particles are 47 nm in size. The prepared nanocomposite is rough and can create a hydrophobic surface. So, due to the use of silica nanoparticles in the nanocomposite, it is more transparent than other models.

The results of the experimental tests also showed that the best pattern is the aluminum surface with cold humidity of 57% at a temperature of 18±2 °C. The more alternating patterns between the surface and the nanocoating, the more water is collected, like in the checkered pattern. Cold humidity helps to collect more water because cold temperatures prevent the collected water from evaporating. Experiments revealed that the patterns' placement angle has a significant effect on air moisture collection, and the higher this angle is higher the amount of water collected will be. The best placement angle is 120°.

CONFLICT OF INTEREST

The authors hereby declare that there is no conflict of interest.

ACKNOWLEDGEMENT

Purpose: This study aimed to identify the dimensions of the innovative university to provide a model for Islamic Azad University.

NOMENCLATURE

HSW	Hybrid Superwettable
FAS	Fluoro-alkyl silanes
SiO2	Silicon dioxide
WCA	Water Contact Angle
SEM	Scanning Electron Microscopy
FT-IR	Fourier transform infrared
PEA	Poly-Ethyl acrylate
PU	Polyurethane
TEOS	Tetraethyl orthosilicate
MTES	Methyl triethoxysilane
OTES	Octyltriethoxysilane
VTES	vinyltrimethoxysilane
BA	butyl acrylate
MMA	methyl methacrylate
HEMA	2- Hydroxyethyl methacrylate
TBHP	tert-Butyl hydroperoxide
ST	Styrene

REFERENCES

[1] Journal article: Mekonnen M. M.; Hoekstra A. Y. Four Billion People Facing Severe Water Scarcity. Sci. Adv. 2016. https://doi.org/10.1126/sciadv.1500323

[2] A. Shokri, Russ. J. Appl. Chem. 88, 2038 (2015). https://doi.org/10.1134/S10704272150120216

[3] H. Zhang, C. Fei, D. Zhang, and F. Tang, J. Hazard. Mater., 145, 227 (2007). https://doi.org/10.1016/j.jhazmat.2006.11.016

[4] U.S. Environmental Protection Agency, 4-Nitrophenol, Health and Environmental Effects Profile No. 135 (Washington DC, 1980).

[5] 4. A. Verma, A. Kaur Hura, and D. Dixit, Des. Water Treat. 56, 677 (2014). https://doi.org/10.1080/19443994.2014.940390

[6] Aref Shokri. (2019). Employing Sono-Fenton Process for Degradation of 2-Nitrophenol in Aqueous Environment Using Box-Behnken Design Method and Kinetic Study. Russ. J. Phys. Chem. A, 93(2), 243-249. https://doi.org/10.1134/S003602441902002X

[7] Journal article: Kim H.; Yang S.; Rao S. R.; Narayanan S.; Kapustin E. A.; Furukawa H.; Umans A. S.; Yaghi O. M.; Wang E. N. Water Harvesting from Air with Metal-Organic Frameworks Powered by Natural Sunlight. Science 2017.

[8] Journal article: Feron P.; Thiruvenkatachari R.; Cousins A. Water Production through CO2 Capture in Coal-Fired Power Plants. Energy Sci. Eng. 2017.

[9] Journal article: Zhang L.; Wu J.; Hedhili M. N.; Yang X.; Wang P. Inkjet Printing for Direct Micropatterning of a Superhydrophobic Surface: Toward Biomimetic Fog Harvesting Surfaces. J. Mater. Chem. A. 2015.

[10] Journal article: Hou Y. M.; Miao Y.; Chen X. M.; Wang Z. K.; Yao S. H. Recurrent Filmwise and Dropwise Condensation on a Beetle Mimetic Surface. ACS Nano 2014.

[11] Journal article: Huang J. Y.; Lai Y. K.; Pan F.; Yang L.; Wang H.; Zhang K. Q.; Harald F.; Chi L. F. Multifunctional Superamphiphobic TiO2 Nanostructure Surfaces with Facile Wettability and Adhesion Engineering. Small 2014.

[12] Journal article: Zhong L.; Zhu H.; Wu Y.; Guo Z. G. Understanding How Surface Chemistry and Topography Enhance Fog Harvesting Based on the Superwetting Surface with Patterned Hemispherical Bulges. J. Colloid Interface Sci. 2018.

[13] Journal article: Yang X.; Song J.; Liu J.; Liu X.; Jin Z. A Twice Electrochemical-Etching Method to Fabricate Superhydrophobic-Superhydrophilic Patterns for Biomimetic Fog Harvest. Sci. Rep. 2017.

[14] Journal article: Yu Z.; Yun F. F.; Wang Y.; Yao L.; Dou S.; Liu K.; Jiang L.; Wang X. Desert Beetle-Inspired Superwettable Patterned Surfaces for Water Harvesting. Small 2017.

[15] Journal article: Kostal E.; Stroj S.; Kasemann S.; Matylitsky V.; Domke M. Fabrication of Biomimetic Fog-Collecting Superhydrophilic-Superhydrophobic Surface Micropatterns Using Femtosecond Lasers. Langmuir 2018.

[16] Journal article: Mishchenko L.; Khan M.; Aizenberg J.; Hatton B. D. Spatial Control of Condensation and Freezing on Superhydrophobic Surfaces with Hydrophilic Patches. Adv. Funct. Mater. 2013. https://doi.org/10.1002/adfm.201300418

[17] Journal article: Lee J.; Hwang S.; Cho D. H.; Hong J.; Shin J. H.; Byun D. RF Plasma Based Selective Modification of Hydrophilic Regions on Super Hydrophobic Surface. Appl. Surf. Sci. 2017.

[18] Journal article: Zhang D.; Chen F.; Yang Q.; Yong J.; Bian H.; Qu Y.; Si J.; Meng X.; Hou X. A Simple Way to Achieve Pattern-Dependent Tunable Adhesion in Superhydrophobic Surfaces by a Femtosecond Laser. ACS Appl. Mater. Interfaces 2012.

[19] Journal article: Kamegawa T.; Shimizu Y.; Yamashita H. Superhydrophobic Surfaces with Photocatalytic Self-Cleaning Properties by Nanocomposite Coating of TiO2 and Polytetrafluoroethylene. Adv. Mater. 2012. https://doi.org/10.1002/adma.201201037
[20] Journal article: Mahapatra P. S.; Ghosh A.; Ganguly R.; Megaridis C. M. Key Design and Operating Parameters for Enhancing Dropwise Condensation through Wettability Patterning. Int. J. Heat Mass Transfer 2016. https://doi.org/10.1016/j.ijheatmasstransfer.2015.08.106
[21] Journal article: Bai H.; Wang L.; Ju J.; Sun R. Z..; Zheng Y. M.; Jiang L. Efficient Water Collection on Integrative Bioinspired Surfaces with Star-Shaped Wettability Patterns. Adv. Mater. 2014.
[22] Journal article: Zhu H.; Guo Z. G. Hybrid Engineering Materials with High Water Collecting Efficiency Inspired by Namib Desert Beetles. Adv. Funct. Mater. 2014.
[23] Journal article: Lai Y.; Huang J.; Cui Z.; Ge M.; Zahng K. Q.; Chen Z.; Chi L. Recent Advances in TiO2-Based Nanostructured Surfaces with Controllable Wettability and Adhesion. Small 2016.
[24] Journal article: Schemenauer RS, Cereceda P (1994b) Fog collection's role in water planning for developing countries. Wiley Online Lib 18:91-100. https://doi.org/10.1111/j.1477-8947.1994.tb00879.x
[25] Journal article: Golovin K, Boban M, Mabry JM, Tuteja A (2017) Designing self-healing superhydrophobic surfaces with exceptional mechanical durability. ACS Appl Mater Interfaces 9:11212. https://doi.org/10.1021/acsami.6b15491
[26] Journal article: Mohammadi R, Wassink J, Amirfazli A (2004) Efect of surfactants on wetting of super-hydrophobic surfaces. Langmuir 20:9657. https://doi.org/10.1021/la049268k
[27] Journal article: Rao AV, Latthe SS, Mahadik SA, Kappenstein C (2011) Mechanically stable and corrosion resistant superhydrophobic sol-gel coatings on copper substrate. Appl Surf Sci 257:5772-5776. https://doi.org/10.1016/j.apsusc.2011.01.099
[28] Journal article: Wang LF, Dai ZD (2016) Effects of the natural microstructures on the wettability of leaf surfaces. Biosurf Biotribol 2:70-74. https://doi.org/10.1016/j.bsbt.2016.06.001
[29] Journal article: Wang Y, Wang X, Lai C, Hu H, Kong Y, Fei B, Xin JH (2016) Biomimetic Water-Collecting Fabric with Light-Induced Superhydrophilic Bumps. ACS Appl Mater Inter 8:2950-2960. https://doi.org/10.1021/acsami.5b08941
[30] Journal article: Dorrer C, Rühe J (2008) Mimicking the stenocara beetle-dewetting of drops from a patterned superhydrophobic surface. Langmuir 24:6154-6158. https://doi.org/10.1021/la800226e
[31] Journal article: Moazzam P, Tavassoli H, Razmjou A, Warkiani ME, Asadnia M (2018) Mist harvesting using bioinspired polydopamine coating and microfabrication technology. Desalination 429:111-118. https://doi.org/10.1016/j.desal.2017.12.023
[32] Journal article: Azad MA, Krause T, Danter L, Baars A, Koch K, Barthlott W (2017) Fog collection on polyethylene terephthalate (PET) fibres: influence of cross-section and surface structure. Langmuir 33:5555- 5564. https://doi.org/10.1021/acs.langmuir.7b00478
[33] Journal article: Weinman CJ, Finlay JA, Park D, Paik MY, Krishnan S, Sundaram HS, Dimitriou M, Sohn KE, Callow ME, Callow JA, Handlin DL, Willis CL, Kramer EJ, Ober CK (2009) ABC triblock surface-active block copolymer with grafted ethoxylated fluoroalkyl amphiphilic side chains for marine antifouling/fouling release applications. Langmuir 25:12266-12274. https://doi.org/10.1021/la901654q
[34] Journal article: Sundaram HS, Cho Y, Dimitriou MD, Weinman CJ, Finlay JA, Cone G, Callow ME, Callow JA, Kramer EJ, Ober CK (2011) Fluorinefree mixed amphiphilic polymers based on PDMS and PEG side chains for fouling release applications. Biofouling 27:589. https://doi.org/10.1080/08927014.2011.587662
[35] Journal article: Zhang H, Nie H, Yu D, Wu C, Zhang Y, Whithe CJB (2010) Surface modification of electrospun polyacrylonitrile nanofiber towards developing an affinity membrane for romelain adsorption. Desalination 256:141-147. https://doi.org/10.1016/j.desal.2010.01.026
[36] Journal article: Zhu H, Guo Z (2016) Hybrid engineered materials with high water-collecting efficiency inspired by Namib Desert beetles. Chem Commun 52:6809-6812. https://doi.org/10.1039/C6CC01894G
[37] Journal article: Kostal E, Stroj S, Kasemann S, Matylitsky V, Domke M (2018) Fabrication of biomimetic fog-collecting superhydrophilic-superhydrophobic surface micropatterns using femtosecond lasers. Langmuir 34:2933-2941. https://doi.org/10.1021/acs.langmuir.7b03699
[38] Journal article: Malik FT, Clement RM, Gethin DT, Krawszik W, Parker AR (2014) Nature's moisture harvesters: a comparative review. Bioinspir Biomim 9:031002. https://doi.org/10.1088/1748-3182/9/3/031002
[39] Journal article: Park KC, Kim P, Grinthal A, He N, Fox D, Weaver JC, Aizenberg J (2016) Condensation on slippery asymmetric bumps. Nature 531:78-82. https://doi.org/10.1038/nature16956
[40] Journal article: Dolatzadeh, F and Moradian, S and Jalili, M.M,1388, effect of Nano Silica on Moisture Absorption of Polyurethane Clear Coats as Studied by EIS and Gravimetric Methods,03rd International Color and Coatings Congress,Tehran,https://civilica.com/doc/71394
[41] Journal article: Wang, S., Yu, X., & Zhang, Y. (2017). Large-scale fabrication of translucent, stretchable and durable superhydrophobic composite films. J. Mater. Chem. A, 5(45), 23489-23496. https://doi.org/10.1039/C7TA08203G
[42] Journal article: P. Król, Synthesis methods, chemical structures and phase structures of linear polyurethanes. Properties and applications of linear polyurethanes in polyurethane elastomers, copolymers and ionomers, Prog. Mater. Sci. 52 (2007) 915-1015. https://doi.org/10.1016/j.pmatsci.2006.11.001
[43] Journal article: A. Darvish, R. Naderi, M.M. Attar, the impact of pigment volume concentration on the protective performance of polyurethane coating with second generation of phosphate-based anticorrosion pigment, Prog. Org. Coat. 77 (2014) 1768-1773. https://doi.org/10.1016/j.porgcoat.2014.05.025
[44] Journal article: H.-M. Kim, J. Lee, J. Seo, J.-H. Seo, Methylsilicone-functionalized superhydrophobic polyurethane porous membranes as antifouling oil absorbents, Colloids Surf. A Physicochem. Eng. Asp. 572 (2019) 47-57. https://doi.org/10.1016/j.colsurfa.2019.03.073
[45] Journal article: F. Carreño, M.R. Gude, S. Calvo, O. Rodríguez de la Fuente, N. Carmona, Synthesis and characterization of superhydrophobic surfaces prepared from silica and alumina nanoparticles on a polyurethane polymer matrix, Prog. Org. Coat. 135 (2019) 205-212.

https://doi.org/10.1016/j.porgcoat.2019.05.036
[46] Journal article: E. Yousefi, M.R. Ghadimi, S. Amirpoor, A. Dolati, Preparation of new superhydrophobic and highly oleophobic polyurethane coating with enhanced mechanical durability, Appl. Surf. Sci. 454 (2018) 201-209. https://doi.org/10.1016/j.apsusc.2018.05.125
[47] Journal article: C. Koti Reddy, D. Shailaja, Improving hydrophobicity of polyurethane by PTFE incorporation, J. Appl. Polym. Sci. 132 (2015).https://doi.org/10.1002/app.42779
[48] Journal article: C. Pereira, C. Alves, A. Monteiro, C. Magén, A.M. Pereira, A. Ibarra, M.R. Ibarra, P.B. Tavares, J.P. Araújo, G. Blanco, J.M. Pintado, A.P. Carvalho, J. Pires, M.F.R. Pereira, C. Freire, Designing novel hybrid materials by one-pot Co-condensation: from hydrophobic mesoporous silica nanoparticles to superamphiphobic cotton textiles, ACS Appl. Mater. Inter. 3 (2011) 2289-2299. https://doi.org/10.1021/am200220x
[49] Journal article: H. Jin, X. Tian, O. Ikkala, R.H.A. Ras, Preservation of superhydrophobic and superoleophobic properties upon wear damage, ACS Appl. Mater. Interfaces 5 (2013) 485-488. https://doi.org/10.1021/am302541f
[50] Journal article: Chen, Y.-C., Zhou, S.-X., Yang, H.-H., & Wu, L.-M. (2006). Interaction and Microstructure of Polyurethane/Silica Hybrid Films Prepared by Sol-Gel Process. J. Sol-Gel Sci. Technol. 37(1), 39-47. https://doi.org/10.1007/s10971-005-4509-9
[51] Journal article: Luo, Z., Shi, Y., Zhao, D., & He, M. (2011). Synthesis of Epoxidatied Castor Oil and Its Effect on the Properties of Waterborne Polyurethane. Procedia Engineering, 18, 31-36. https://doi.org/10.1016/j.proeng.2011.11.006
[52] Journal article: Yu, F., Gao, J., Liu, C., Chen, Y., Zhong, G., Hodges, C., … Zhang, H. (2020). Preparation and UV aging of nano-SiO2/fluorinated polyacrylate polyurethane hydrophobic composite coating. Prog. Org. Coat. 141, 105556. https://doi.org/10.1016/j.porgcoat.2020.105556
[53] Journal article: Luo, G., Jin, Z., Dong, Y., Huang, J., Zhang, R., Wang, J., Zhang, L. (2016). Preparation and performance enhancements of wear-resistant, transparent PU/SiO2 superhydrophobic coating. Surf. Eng., 34(2), 139-145. https://doi.org/10.1080/02670844.2016.1236068
[54] Journal article: Zhou, Y., Liu, C., Gao, J., Chen, Y., Yu, F., Chen, M., & Zhang, H. (2019). A novel hydrophobic coating film of water-borne fluoro-silicon polyacrylate polyurethane with properties governed by surface self-segregation. Prog. Org. Coat.134, 134-144. https://doi.org/10.1016/j.porgcoat.2019.04.078
[55] Journal article: Wei, X., & Zhang, F. (2018). Surface and mechanical properties of an organic-inorganic super-hydrophobic coating using modified nano-SiO2 and mixing polyurethane emulsion as raw materials. J. Adhes. Sci. Technol. 32(16), 1809-1821. https://doi.org/10.1080/01694243.2018.1449574
[56] Journal article: Zhai, L., Liu, R., Peng, F., Zhang, Y., Zhong, K., Yuan, J., & Lan, Y. (2012). Synthesis and characterization of nanosilica/waterborne polyurethane end-capped by alkoxysilane via a sol-gel process. J. Appl. Polym. Sci. n/a-n/a.
[57] Journal article: Nørgaard, T., & Dacke, M. (2010). Fog-basking behaviour and water collection efficiency in Namib Desert Darkling beetles. Front. Zool. 7(1), 23. https://doi.org/10.1186/1742-9994-7-23
[58] Journal article: Hai Zhuab, Zhiguang Guo and Weimin Liub, Biomimetic water-collecting materials inspired by nature. Chem. Commun. 2 (2012).
[59] Journal article: Feng, J., Zhong, L., & Guo, Z. (2020). Sprayed hieratical biomimetic superhydrophilic-superhydrophobic surface for efficient fog harvesting. Chem. Eng. J. 388, 124283. https://doi.org/10.1016/j.cej.2020.124283